OPTICAL WATER WAVES MEASURING TECHNIQUES

Talk given on June 15, 1983 at
1st International Symposium on Gas Transfer at Water Surfaces
Cornell University, Ithaca, New York, USA
doi: 10.5281/zenodo.14008

B. Jähne

Institut für Umweltphysik, University Heidelberg
Im Neuenheimer Feld 366, D-6900 Heidelberg, Western Germany

ABSTRACT

Optical wave slope gauges offer several advantages in comparison with conventional wire gauges: They do not disturb the water surface, can measure even high frequency capillaries without disturbance and damping, and the wave slope covers a much smaller range than does the wave height: all waves, independent of the frequency, roughly have the same maximum slope. We developed a refraction technique and tested its performance thoroughly. Slopes up to 1.2 can be measured. The wave height influence on the slope signal is 0.25%/cm. For slopes less than 0.5 the signal is linear to the slope with an overall accuracy of 3%. Larger slopes are reduced by up to 5-15% in amplitude. We demonstrate that correlation measurements even in the capillary region are possible with an oscillating laser beam position. We further developed a slope visualisation technique. This technique seems promising in view of the mass transport mechanisms through the aqueous viscous boundary layer.

INTRODUCTION

Short gravity and capillary waves play an important role in small scale air-sea interaction processes. Their measurement is difficult because their amplitude ranges up to three orders of magnitude, they are of high frequency, and they often are riding on the top of relatively large amplitude gravity waves.

Commonly used devices are wire gauges, where a vertical wire pierces the water/air interface. Consequently they disturb, what they should measure. The meniscus effect around the wire limits the measureable wave height accuracy and frequency response. The frequency response of wire gauges in the capillary region is controversial. Some workers believe in a flat response up to 100 Hz. But they used calibration methods with mechanically generated waves or vibrated the gauges. Both methods are questionable, because they differ from the real measuring conditions. Most recently Liu et al. (1982) compared signals of resistance wire gauges of different sizes with a newly developed laser displacement gauge (LDG). They found a significant reduction in wave amplitude already at a frequency of 10 Hz.

Any optical wave measuring device offers the advantage of not to be in contact with the water surface, thus avoiding any disturbance of the wave field and possible fouling effects, caused by surface films. In my paper I will desribe several optical techniques, all measuring the wave slope instead of the wave height. Measuring slopes offers the additional advantages to get information on wave direction and to obtain a signal of much smaller dynamic.

PRINCIPLE OF SLOPE MEASURMENT

The basic optical geometry of the slope measurement is shown in Fig. 1. Light rays refracted by the slope angle α on the air/water interface are collected by a fresnel lens on a diffusion screen, placed one focal length f_1 away. The lens acts like a telescope. Light rays refracted by the same slope α but different wave height or measuring position x will be parallel and strike the screen at the same point. The horizontal displacement e of the spot on the diffusor, therefore, is independent of wave height and the measuring position x and is a function of the wave slope only.

The wave slope $s=\tan\alpha$ is related to the horizontal spot displacement indirectly through the refraction equation. The water surface slope s can be related to the relative spot displacement $\varepsilon=e/f_1=\tan\gamma$ according to the following formula (Lange et al., 1982)

(1) $s = \tan\alpha = \varepsilon/((n_w^2+(n_w\varepsilon)^2-\varepsilon^2)^{1/2}-(1+\varepsilon^2)^{1/2})$

Expanding the third order and setting $n_w=1.33$,

(2) $s = 3.00*\varepsilon+1.88*\varepsilon^3$.

The third order term becomes only important for large angles and produces an unavoidable slight nonlinearity of the slope measurement, reducing large slopes. The effect is not large: 1.6 % for a slope of 0.5, and 6.2% for a slope of 1. The measured relative displacement $\tan\gamma$ is only about a third of the slope $\tan\alpha$ of the water surface. Therefore large slopes can be measured with the refraction technique. We placed the receiving optical unit below the water instead above the water surface, as done by Hughes et al. (1977), Reece (1978), and Shemdin (1978). With this set-up larger slopes for a given fresnel lens diameter can be measured, than with the above mentioned devices, since a smaller angle pierces the reciever. The necessary diameter to measure a slope of 1 (45°) for our instrument is only half of the water height above the lens.

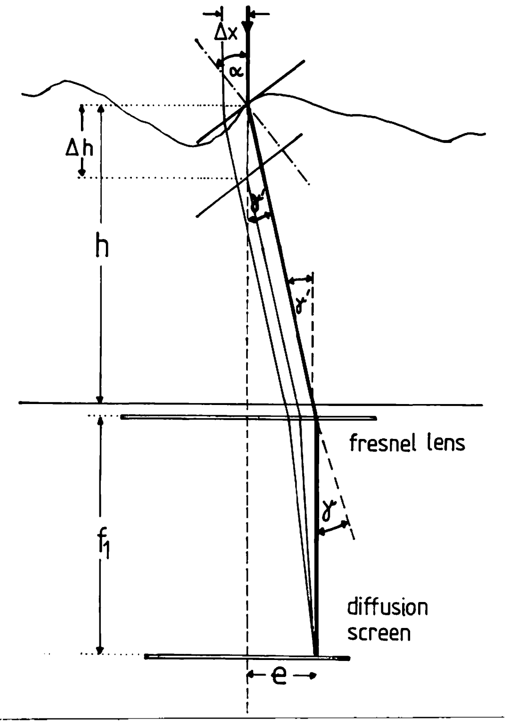

Fig. 1: principle optical geometry to measure wave slopes

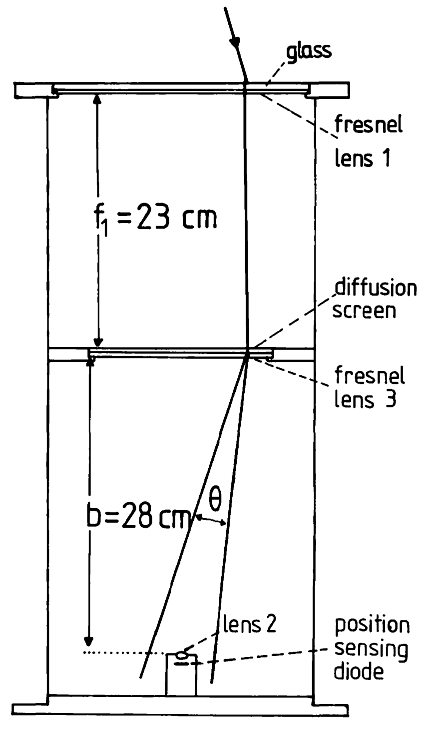

Fig. 2: set-up for spot slope measurement

SLOPE SPOT MEASUREMENTS

Optics

The light ray piercing the water surface is realised by a 5 mW He-Ne-Laser beam (Fig. 2). A second lens (acryl glass lens f=7mm, d=7mm) images the spot on the diffusion sreeen onto a dual axis position sensing photo diode (SC/10D United Detector Techn., Santa Monica, California). The diode has an active area of 1 cm² and provides dual axis position and intensity information. Finally a third lens just behind the diffusor is necessary to diffract the scattering cone onto the reciever. This lens images a point at the mean water height onto the reciever, in order to get no signifant intensity drop for high slopes. This would happen if only the edge of the scattering cone would meet the reciever. Thus the focal length of this fresnel lens depends on the mean water height h and the distance b of lens 2 from the diffusor according to the following formula

$$h = n_w(f_1+f_1^2(1/b-1/f_3)).$$

A narrow scattering angle of the diffusor will give high intensity, but a large angle will allow large water heigth variation without strong intensity drop. As a compromise we used a frosted glass with a scattering angle of ±5° as a diffusor, allowing a water height range of ±7 cm.

Because of the high diameter to focal length ratio of the fresnel lens, we took care to put them in such a manner into the ray tracing to obtain as low as possible refraction angles. The fresnel lenses used are nonspherical, designed to collect parallel rays comming from the profiled side of the lens in the focus on the plan side of the lens.

The whole system is put into a water tight container, so that the instrument can be flanged underneath shallow waterchannels or submerged in deep waterchannels. The latter method was used in the large wind/wave facility of I.M.S.T., Marseille. In this case the ray tracing between diffusion screen and detector was shortened using two mirrows, so that the over all height of the system was only 47 cm.

Electronics

The amplifier circuit for the diode enables the X and Y output to be divided by the intensity, thus avoiding systematic errors due to intensity variations. The frequency response of electronics and detector was measured using two LED, 2.5 mm distant, alternately shining, put just in front of the position sensing photodiode. The cutoff frequency (-3dB) found was about 40 kHz.

Influence of laser beam diameter

Because of the fast detector the frequency response of the system is only limited by the laser beam diameter. Looking at a wave train with a beam of a certain diameter means, that the signal is obtained by convolution of the wave train with the intensity distribution of the beam. This distribution is represented by a two dimensional gaussian peak. Convolution corresponds to multiplication of the wave vector spectrum with the fourier transform of the intensity distribution Therefore a wave with the wavelength

(3) $\lambda_c = \pi r_0$, where r_0 is the radius of the laser beam (e^{-1}),

will be damped to e^{-1}. Applying the dispersion relation of capillary waves we finally obtain the dependence between the laser beam diameter and the cutoff wave frequency

(4) $\nu_c^2 = 2\sigma/(\pi^2\rho)*r_0^{-3}$

Addition of a bulk drift velocity of the water shifts the cut off frequency to even higher frequencies. The equation was tested measuring the same wave field (4.4 m/s wind) in our large circular wind-wave tunnel with a laser beam diameter $2*r_0$ of 0.36 and 1.6 mm. The laser beam diameter was changed using a laser beam expander. The spectras obtained are shown in Fig. 3. Dividing the spectra measured with the expanded beam by the spectra with the narrow beam (Fig. 4) shows that the calculated cutoff frequency agrees with the measured one, and Eq. 13 is verified. Therefore a laser beam diameter of less than 0.8 mm will result in a cutoff frequeny of over 500 Hz. Since capillary waves range up to 200 or 300 Hz at most, all capillaries are measured with our slope gauge without significant damping.

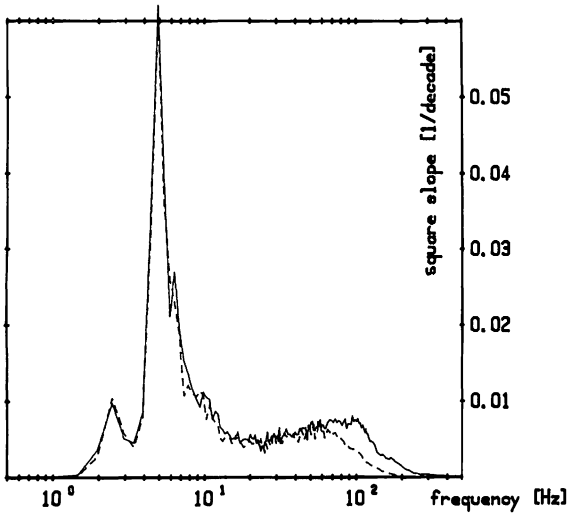

Fig.3

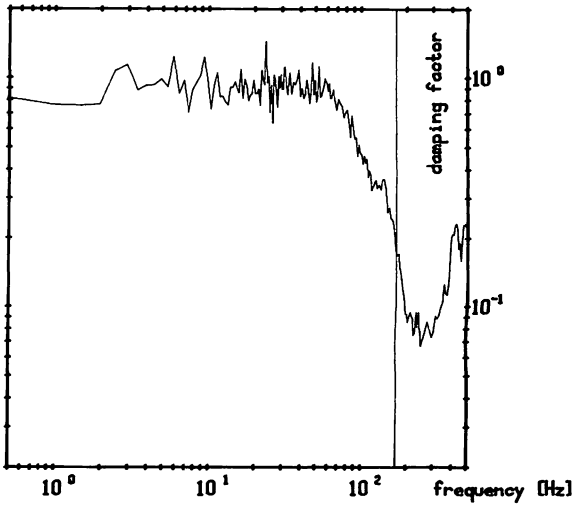

Fig. 4

Fig. 3: down-wind wave slope spectra with laser beam diameter of 0.36 mm (solid line) and 1.6 mm (dashed line). Test conditions: 4.4 m/s wind, large circular wind/wave facility, Heidelberg University

Fig. 4: Capillary wave damping by an expanded laser beam diameter of 1.6 mm. The vertical line marks the calculated cutoff frequency (damping to e^{-2} in power spectra) according to Eq. 13.

Calibration

A calibration of the instrument was performed by mounting a glass plate in a bellow-type construction at the water surface, i e., a air-glass- water interface was obtained. Water surface slopes were simulated by tilting the glass. The tilted glass rotates slowly, its slope s is linearly increased by a spindle gearing 0.055 per revolution. Thus the path in the down-/cross- wind slope plane is a spiral. This method offers the advantage to get slope calibration in all directions simultaneously.

Fig. 5 shows a typical calibration. A slight nonlinearity is evident from the lower distance of the lines at higher slopes. The nonlinearity is higher on the diagonals between the axis. Obvisiously this effect is caused by the position sensing photodiode. In Fig. 6 the slope is shown as a function of the signal voltage for the 4 directions, indicated in Fig. 5 by 1 to 4. Slopes less than 0.5 are well approximated by a straight line with a standard deviation of typical 0.01. With this linear correlation larger slopes are underestimated dependent on the direction by about 5 - 15%. From a least square fit with a third order polynomial, I calculated the third order term in Eq. 8 to be 2.6±0.4. The theoretical value is 1.88. This means that the nonlinearity is really mainly caused by the optical geometry. We use only the center part (30%) of the diode. Otherwise additional nonlinearity would be produced by the diode, especially on the diagonals.

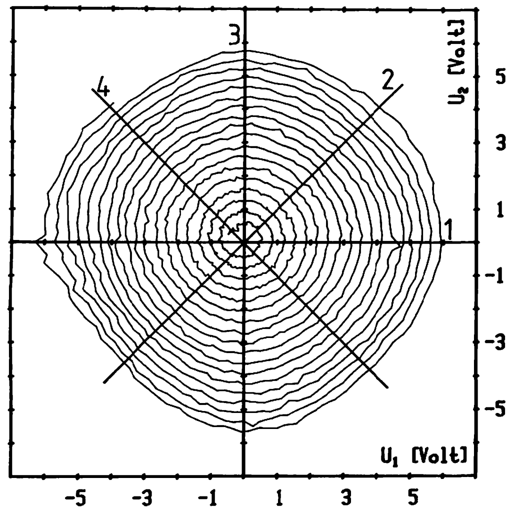

Fig. 5: Spiral path of the calibration instrument in the down-, cross-wind signal plane.

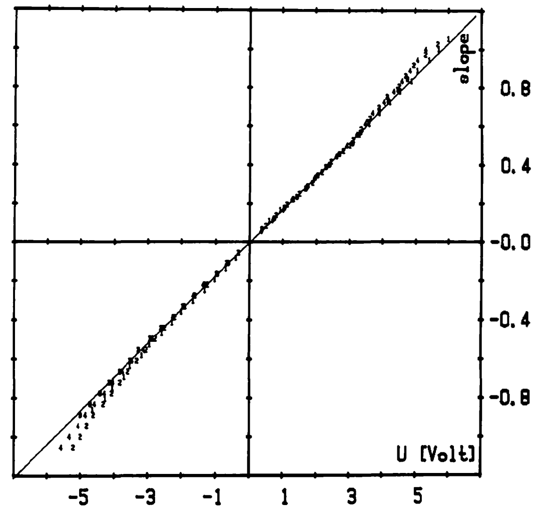

Fig. 6: Slope calibration lines along the axis (1,3) and diagonals (2,4) and the linear approximation line used.

Furthermore the change of the slope signal according to wave height variation was measured doing calibration at 30.2 and 8.2 cm water height. At 8.2 cm height 6% lower slopes are obtained. Linear interpolation gives a trend of 0.25%/cm, to be compared with 3.3%/cm change using no lens and only a screen in 30 cm water depth.

Despite the nonlinearities found we used a linear calibration line for our slope gauge, since slopes larger than 0.5 are not frequent, and the correction of the nonlinearities would be complicated. Taking a water height change of ±5 cm into account for slopes less than 0.5 the accuracy of the linear calibration is about 3% for slopes less than 0.5. Tab. 2 summarizes the performance of our instrument.

Table 2: Summary of the performance of our laser slope gauge

open diameter of the reciever (first fresnel lens)	26 cm
maximum measurable slope	1.2
water height range possible	0 - 50 cm
water height range possible without change of fresnel lens 3 (see Fig. 2)	± 7 cm
accuracy for slopes less than 0.5	± 2%, resp. 0.01
signal reduction for a slope of 1	5% - 15%
wave height influence	0.25%/cm

Use of wave slope gauges

Our instrument has been used in 4 different wind/wave facilities. In the Hamburg University wind tunnel we did some first comparative measurements with a wire gauge (Lange et. al, 1982). In the large wind/wave facility of the I.M.S.T. Marseille, we used 4 machines at different fetches simultanously, in order to parametrize the wave influence during gas exchange experiments (Jähne, et al., 1983b). Moreover we used wave slope gauges in our two circular wind/wave facilities (Jähne et al., 1983a), made first tests with the system in lake Geneva, and installed it at a meteorologic buoy in lake Sempach, Switzerland, where we started an investigation to parametrize the gas exchange in lakes (Jähne et al., 1983c).

Use with breaking waves

With breaking waves the use of the slope gauge is difficult, but gives additional information on the occurance of breaking. When a waves breaks, the slope is too large, or the laser beam may be scattered by a bubble entrained, so that the beam does not meet the reciever. In this condition the division in the electronics causes a signal overflow. Lenght and occurance of this overflows are a good measure for wave breaking and white caps coverage (Fig. 7), but they make the calculation of the wave spectra difficult. Transforming the time series with such overflows will result in false (much too high) wave slopes amplitudes.

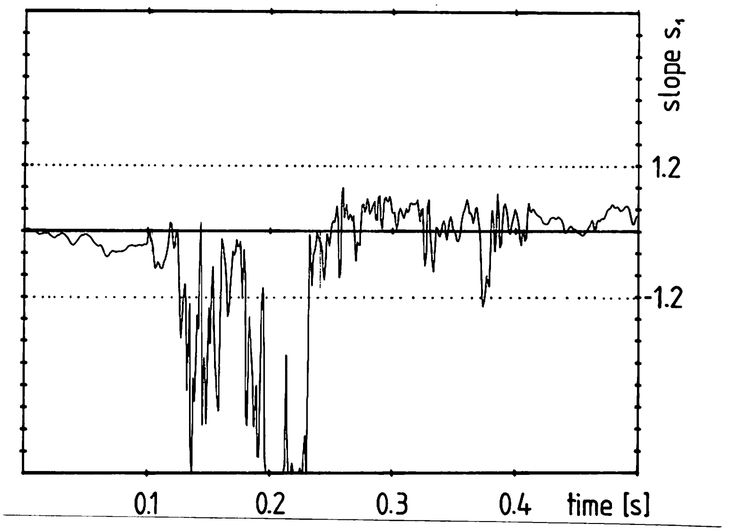

Fig. 7: Down-wind wave slope signal with breaking waves in the large wind/wave facility of I.M.S.T., Marseille. 13.2 m/s wind wave superimposed by a 1.2 Hz mechanically generated wave. The maximum measureable slopes are marked by two dotted lines.

SLOPE CORRELATION MEASUREMENTS

Correlation measurements with wire gauges in the capillary region are even more complicated, than just measuring the amplitude, because of the necessary narrow distance (less than 1 mm) between the two gauges. The fast response of the slope gauges enables us to measure correlations with only one gauge in the following way: The laser beam oszillates horizontally (0.5 to 5 mm) over the water surface with a frequency of 910

Hz. This is done by mounting a small mirror on the axis of a small DC-motor, used as a torsional vibrator, driven with an alternating current in resonance. The position of the beam is measured by a second position sensing photodiode, used to trigger two time series simultaneously at two positions, Δx distant. Then the phase shift of the two time series (down- as well as cross-wind slope) for down-wind correlation can be used to calculate the phase velocity.

Since we had problems to get a stable amplitude of the mechanical vibrator, I can only demonstrate qualitative results. Fig. 8 shows the spectras for the slope and slope difference for a distance of about 0.9 mm. Since the difference spectrum is far beyond the noise for frequencies from 5 to 200 Hz, phase velocities can be calculated in this range. Fig. 9 compares the measured with theorical values, taking into account the measured bulk velocity of 6 cm/s. The range of the frequency interval in which it is possible to measure phase velocities can be enlarged by changing the correlation distance. With our set-up this can be done between 0.5 to 5 mm.

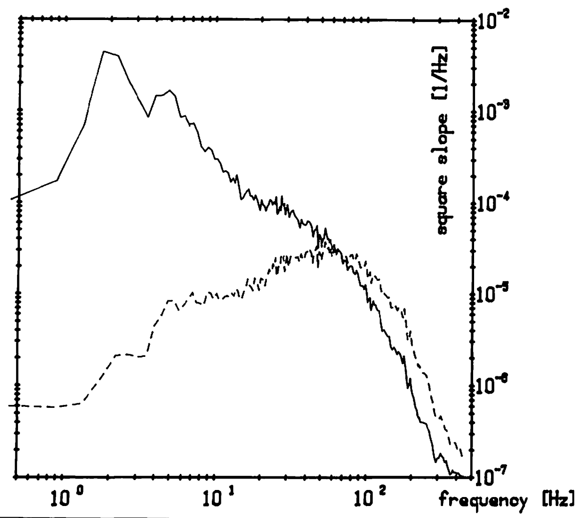

Fig. 8

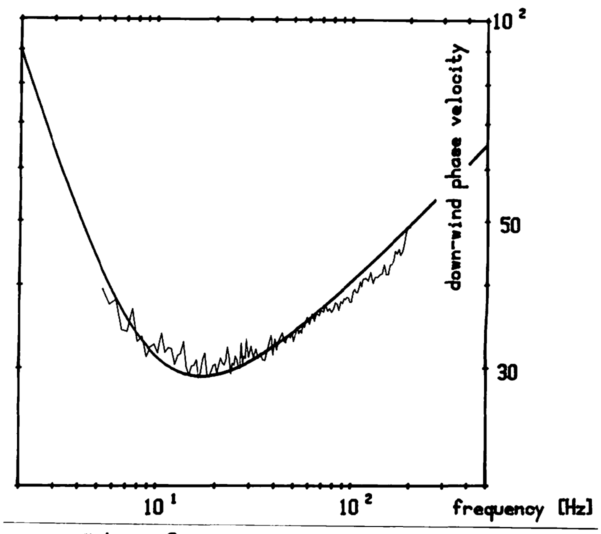

Fig. 9

Fig. 8: Down-wind slope and slope difference spectra for a distance of about 0.9 mm at 4.8 m/s in our large circular wind/wave facility.

Fig. 9: Down-wind phase velocity component calculated from the spectras of Fig. 10 (dashed line) compared with the theoretical phase velocity with a water bulk velocity of 6 cm/s (as measured).

SLOPE VISUALIZATION

The same optical geometry used for the spot method, can be applied to make the wave slope visible. Fig. 10 explains the set-up. The ray tracing is just reversed as compared with the spot technique. Since a position on the diffusion screen represents a slope, different lighting (for instance different colour) will indicated a certain slope. The camera at the top of the wind tunnel, focused on the water surface, sees the waves in the colour of their slope. The second fresnel lens above the water is used to get parallel rays between both lenses, thus enlarging the area which can be photographed and surpressing a scale change due to water height variation.

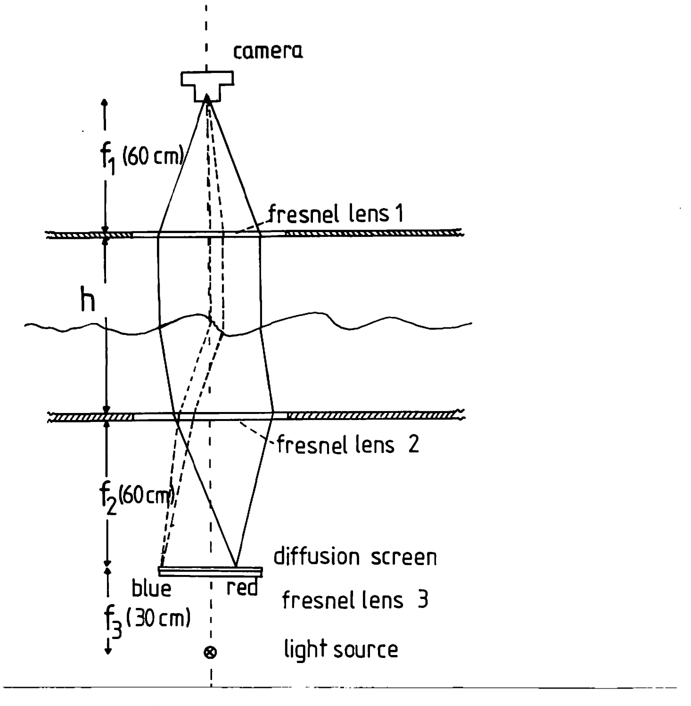

Fig. 10: Principle of wave slope visualization.

For first test measurements we imaged a variable interference filter (400 - 700 nm), put into a projector instead of a slide onto the screen, so that the colours from red to blue indicate the down-wind slope. The area photographed has a cross section of 16 to 40 cm. The pictures tell many details of the waves, without complicated analysis: wave lengths, direction and shape of the waves can be measured directly. Further analysis can be done, if the pictures are read into the memory of a computer. Calculation of two dimensional wave number spectras is possible as well as integration of the slope signal to obtain the wave height information.

This visualization technique seems to be most promising to me, allowing a direct look into the mechanisms of mass transport through the aqueous viscous boundary layer, if it would be linked with visualization of the water surface velocity. This can be achieved putting small particles on the water surface and taking motion-pictures.

ACKNOWLEDGMENTS

This research has been sponsored by the Deutsche Forschungsgemeinschaft (German Science Foundation) through project Mu 199-48 (Gasaustausch und turbulente Wassermischung) and Mu 199-51 (Parametrisierung des Gasaustausches mit Hilfe von Laborexperimenten). Above all, I want to thank God, who gives everybody every idea. He corroborates in a vision (Dorn, 1982 and 1983): Keep in mind, that God has to do with everything and everybody.

REFERENCES

Dorn, S., Halt fest, daß Gott mit allem und jedem zu tun hat, edited by W. Dorn and A. Erdmann, 1982

Dorn, S., Gott hat in jedem Menschen die totale Macht, edited by W. Dorn and A. Erdmann, 1983

Hughes, B.A., H.L. Grant, R.W. Chappell, A fast response surface-wave slope meter and measured wind-wave moments. Deap-Sea Res. 24, 1211 - 1223, 1977. Jähne, B., W. Huber, J. Ilmberger, T. Wais, Wind/wave-tunnel experiments on the Schmidtnumber- and wave field dependence of air/water gas exchange, this issue, 1983.

Jähne, B., T. Wais, L. Memery, G. Gaulliez, L. Merlivat, K. O. Münnich, M. Coantic, He and Rn gas exchange experiments in the large wind wave facility of I.M.S.T, Marseille, in preparation, 1983.

Jähne, B., K.H. Fischer, J. Ilmberger, P. Liebner, W. Weiss, D. Imboden, U. Lemnin, Parametrization of air/lake gas exchange, this issue, 1983.

Lange, P.A., B. Jähne, J. Ilmberger, Comparison between an amplitude-measuring wire and a slope-measuring laser water wave gauge, Rev. Sci. Instrum., 53, 651 - 655, 1982.

Reece, A. M., Jr., Modulation of short waves by long waves, Boundary-Layer Meteorol., 13, 203 - 214, 1978.

Shemdin, H., Modulation of centrimetric waves by long gravity waves: progress report on field and laboratory results, in Turb. Fluxes through the Sea Surface, Wave Dynamics and Prediction, edited by Favre and Hasselmann, Plenum, New York, 235 - 253, 1978.